Prescission neutron emission in $^{235}U(n_{th},f)$ through fragment-neutron angular correlation studies

M.S. Samant,* R.P. Anand, R.K. Choudhury, S.S. Kapoor, and D.M. Nadkarni
Nuclear Physics Division, Bhabha Atomic Research Centre, Bombay 400 085, India
(Received 15 December 1994)

Measurements of prompt neutron energy spectra and angular distributions from mass and kinetic energy selected fission fragments were carried out in the thermal neutron fission of ^{235}U. Neutron energy was determined by the time-of-flight technique and fission fragment energy and angle were measured using a back-to-back gridded ionization chamber. The measured angular distributions of neutrons emitted from fragment pairs of various mass and kinetic energy were compared with results of Monte Carlo calculations assuming neutron emission from fully accelerated fragments to determine the component of neutrons which may be emitted in the prescission stage. The calculations were carried out using as inputs the measured center-of-mass neutron energy spectra and multiplicities and assuming isotropic emission of neutrons in the center-of-mass frame of both the fission fragments, and a three source fitting of the angular distributions was done to deduce the component of prescission neutrons. The value of the prescission neutron multiplicity averaged over all fragment masses is found to be 0.25 ± 0.05 (about 10% of the total neutron multiplicity). The present results have been discussed on the basis of the energy damping and time scale of the saddle to scission transition in the thermal neutron induced fission process.

PACS number(s): 25.85.Ec, 21.60.Ka, 24.75.+i

I. INTRODUCTION

It is now well established that in low energy fission the prompt neutrons are emitted primarily from fully accelerated fragments and are, therefore, strongly correlated with the direction of motion of fission fragments as expected from kinematic considerations. However, there still remains the question whether a small fraction of the neutrons is emitted in the prescission stage during saddle to scission transition. These neutrons will have nearly isotropic angular distribution in the laboratory system and are generally classified as prescission neutrons (ν_{pre}). There is as yet no clear consensus on the number of prescission neutrons emitted in the case of spontaneous fission and low energy fission processes. The yield of prescission neutrons as deduced in earlier studies for $^{235}U(n_{th},f)$ and for spontaneous fission of ^{252}Cf range from 5% to 15% of the total neutron yield [1–12]. Some recent measurements on the neutron anisotropy data [13–15] in the case of $^{252}Cf(sf)$, have given the yield of prescission neutrons to be even less than 5%. An accurate knowledge of the prescission neutron component is crucial for the understanding of the energy dissipation mechanism and saddle to scission time scales in the fission process, and it would also help in refining the models used for calculations of fission neutron spectra. Studies on prompt neutron emission in heavy ion induced fission reactions have clearly estabilished that the observed number of prescission neutrons is, in general, much higher than that expected from statistical models, thereby leading to the conclusion of presence of a dynamical fission delay and/or prolonged saddle to scission transition times in the fission process (for a review see Refs. [16,17]).

Experimentally, the question of whether or not the prescission neutron component is present is answered by comparison of the experimental fragment-neutron angular correlations with calculations based on the assumption of neutron emission only from fully accelerated fragments. The calculated neutron angular distributions are, however, sensitive to the emission spectra of neutrons in the rest frame of fragments, which are used as inputs to the calculations. The large variations in the deduced ν_{pre} values in the earlier studies seem to be connected with the uncertainties in the input spectra used in those calculations. The present work is aimed to carry out a self-consistent analysis by using the experimentally measured neutron spectra in the rest frame of fragments to calculate fragment-neutron angular correlations and compare them with the corresponding experimental correlations to derive information on ν_{pre} as a function of mass and kinetic energy of fragments in thermal neutron induced fission of ^{235}U. The present results show that the value of ν_{pre} averaged over all fragment masses and kinetic energies is 0.25 ± 0.05, which is about 10% of the total neutron multiplicity for the $^{235}U(n_{th},f)$ reaction. It is also observed that ν_{pre} has a very weak dependence on fragment mass but has strong variations with fragment kinetic energy. The details of the experimental setup are given in Sec. II. Section III gives the details of the data analysis procedure and results. The calculation procedure for the determination of ν_{pre} is described in Sec. IV. Section V contains the discussion of the present results with regard

*Present address: Nuclear Reactions Group, Tata Institute of Fundamental Research, Bombay 400 005, India.

 ©1995 The American Physical Society

to the time scale and the energy damping in the fission process.

II. EXPERIMENTAL SETUP

The experiment was carried out at the CIRUS reactor at Trombay using the thermal neutron beam with a flux of about 10^7 neutrons/cm^2/s. Figure 1 shows a schematic diagram of the experimental setup used for the present measurements. A back-to-back gridded ionization chamber [18] was used to measure the energies of the fission fragment pair and also the angle of emission with respect to the electric field direction in the chamber. A NE213 liquid scintillation detector was used for the neutron energy measurements by the time of flight method in coincidence with fission. The ionization chamber consisted of a central cathode and two parallel plate gridded ionization chambers in back-to-back geometry with the cathode-grid and collector-grid distances of 3.0 cm and 0.7 cm, respectively. A ^{235}U target of about 100 μg/cm^2 thickness was electrodeposited on a thin gold coated VYNS backing (gold thickness $\sim$20 μg/cm^2) and was mounted in the center of the cathode. The chamber was filled with P-10 gas at 1.1 atmosphere, so as to stop all the fission fragments in the cathode-grid region. The gas was continuously purified by circulating it over heated calcium filings which ensured long term stability in the performance of the ionization chamber. The NE213 liquid scintillation neutron detector of 5 cm diameter and 5 cm thickness was placed at a distance of 70 cm from the uranium target, along the direction of the electric field of the ionization chamber. The neutron detector was adequately shielded from background neutrons and gamma rays by using 7-cm thick lead and 50-cm thick borated paraffin in a cylindrical geometry. The neutron time of flight was derived by taking the start signal from the common cathode of the ionization chamber and the stop signal from the neutron detector. The pulse shape discrimination property of the NE213 scintillator was used to distinguish between neutron and gamma ray events in the detector. The pulse heights of the signals from the collectors (V_{c1},V_{c2}), the grids (V_{g1},V_{g2}) of the ionization chamber, the pulse shape and energy signals of the neutron detector, and the neutron time of flight were recorded event by event in list mode for further off-line analysis.

III. DATA ANALYSIS AND RESULTS

A total of 3.6×10^6 coincident events were collected out of which about 10^6 events corresponded to coincidence with prompt neutrons. Data were also collected at regular intervals for fission events without coincidence requirement with the neutron detector for calibrating the collector and grid pulse heights of the back-to-back ionization chamber to determine the energy and angle of emission of the fission fragments. The threshold of the neutron detector was set at 60 keV electron equivalent energy by using an ^{241}Am source. This corresponds to a neutron energy threshold of about 200 keV. Neutron events were selected off-line by using a two-dimensional gate on the neutron time of flight and pulse shape of the neutron detector pulses. The time resolution as determined from the prompt gamma ray peak in the time of flight spectrum was seen to be about 2.5 ns (Fig. 2). The efficiency of the neutron detector was determined by comparing the measured ^{236}U fission neutron spectrum in 2π geometry with the known theoretical spectrum shape [19]. The experimentally measured efficiency as a function of neutron energy agreed well with the results of a Monte Carlo calculation for the detector efficiency.

The data without coincidence with neutrons were analyzed to obtain the calibration of the collector pulses V_c into fragment kinetic energy and the grid pulses V_g into fragment angle. The method of analysis for angle determination using the grid and collector pulse heights followed the general procedure reported in the earlier works [18,20], but with further improvements to take into account the fragment energy loss in the target and backing material. Since the V_g/V_c ratio is related directly to the fragment angle, the energy loss corrections to the grid and collector pulse heights (V_g and V_c) were obtained from the observed shifts in the V_c distribution as a function of V_g/V_c ratio. The corrected collector pulse heights were energy calibrated by using the postneutron energies of the heavy and light fragment groups which were taken as 69.8 MeV and 100.1 MeV, respectively. These postneutron energies were obtained after correcting the average preneutron energies of the light and heavy fragments reported by Unik *et al.* [21] for neutron emission effects. The provisional masses of the complementary fragments were first calculated from the measured fragment energies. The preneutron masses and kinetic energies were obtained iteratively after correcting for the prompt neu-

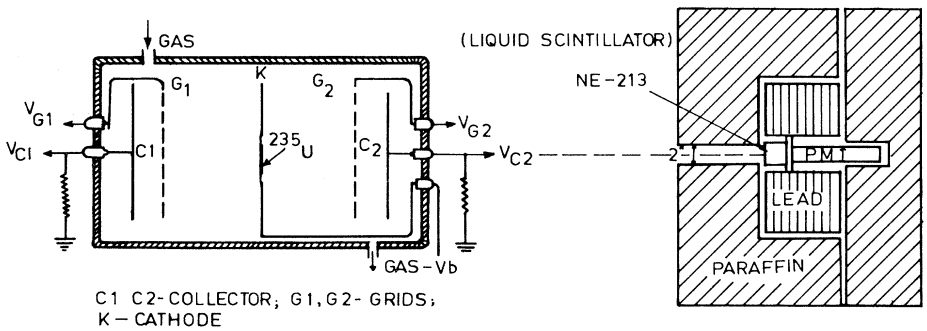

FIG. 1. Schematic diagram of the experimental setup showing the neutron detector sheilding and the back-to-back gridded ionization chamber.

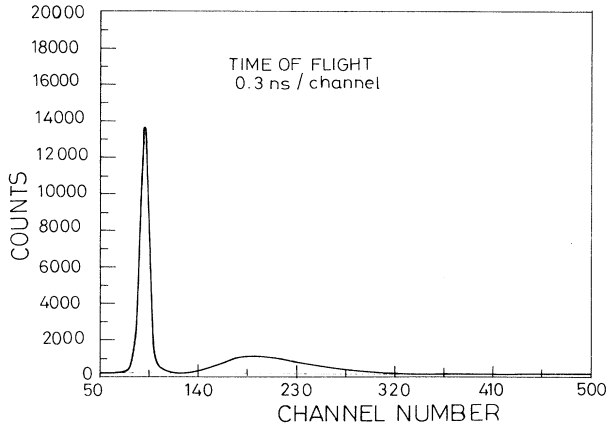

FIG. 2. Time-of-flight spectrum of the prompt neutrons and gamma rays; time resolution obained from the width of the prompt gamma peak is 2.4 ns and the dashed line shows the estimation of the background level under the prompt neutron bump.

tron emission using the experimental data on the $\bar{\nu}$ as a function of mass and total kinetic energy in $^{235}U(n_{th}, f)$ [22] and also for the fragment recoil due to neutron emission [23] in the case of neutron coincidence data.

A. Fragment angle determination

Figure 3 shows the typical grid pulse height distributions for the singles events obtained after correcting for the fragment energy loss as described above. As expected for an isotropic emission, the grid pulse height distribution for fixed mass and kinetic energy bin has a rectangular shape, with the lower and upper edges corresponding to 0° and 90° angles. The 0° and 90° channel numbers were determined for each mass and kinetic energy bin using the criterion described in Ref. [18], and were fitted separately with second order mass and energy dependent polynomial functions as given in Ref. [20]. Using these calibration constants, the fission fragment angle could be determined event by event from the measured V_g and V_c pulse heights. A more detailed description of the present analysis method for the energy and angle measurements has been published earlier [24]. The angular resolution of this method, as determined from the difference between the angles of the complementary fission fragments measured on the two sides of the ionization chamber, was seen to correspond to a FWHM of 3° to 5°. With the present analysis technique, the fragment angle could be accurately determined over the complete 2π angular range except for events corresponding to fragment emission within a few degrees to the target foil (energy loss greater than 10 MeV). The angular distribution could therefore be measured continuously over angles $0° \leq \Theta \leq 87°$ with respect to the electric field direction of the ionization chamber.

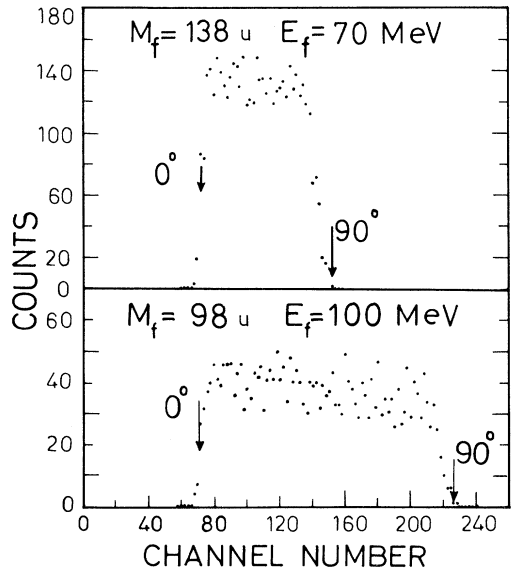

FIG. 3. Grid pulse height distribution for the most probable mass pair of $M_L = 96$ and $M_H = 140$ for unit mass and energy bin; the positions of the 0° and 90° angle calibarations are shown by arrows.

B. Neutron energy spectra and multiplicities

The center-of-mass neutron energy spectra were determined by analyzing the neutron coincidence events, corresponding to fragment emission in a cone of half angle ±18° with respect to the direction of neutron emission. Due to strong kinematic focusing of neutrons by the fragment motion, it can be assumed that the neutrons detected at an angle close to the direction of fragment motion correspond to emission predominantly from the fragment moving towards the neutron detector. A very small fraction (less than a few percent) of the neutrons emitted from the complementary fragment moving in the opposite direction, which may appear in the forward cone of the fragment moving towards the neutron detector, will have very low energy close to the neutron detector threshold. Thus the observed neutron energy can be transformed event by event to center-of-mass neutron energy η by simple kinematic transformation involving the energy per nucleon of the emitting fragment. Following the above procedure the center-of-mass energy spectra of neutrons were obtained as a function of various fragment mass and kinetic energy bins. These spectra were determined after correcting for the efficiency of the neutron detector and also subtracting the background contributions as estimated from the time of flight spectrum. The center-of-mass neutron energy spectra thus obtained were fitted with the expression corresponding to the shape of the neutron evaporation spectrum [14] given by

$$N(\eta) = \text{const}\sqrt{\eta}\exp(-\eta/T_{\text{eff}}) \ , \qquad (1)$$

where η is the center-of-mass neutron energy and T_{eff} is an effective temperature parameter. The T_{eff} values were

determined from the above fits as a function of total kinetic energy (E_K) for various fragment mass bins (M_f). The neutron multiplicity ($\overline{\nu}$) per fragment was obtained by integrating over energy the neutron yield per fission and after correcting for the kinematic focusing effects due to fragment motion. The results on $\overline{\nu}$ and T_{eff} as a function of E_K and M_f have been reported in an earlier publication (Figs. 4 and 5 of Ref. [25]). The T_{eff} and $\overline{\nu}$ are seen to generally decrease with the fragment kinetic energy for all the fragment mass bins. These results were discussed in detail in Ref. [25] to provide information on the temperature and level density parameter of the neutron rich fragment nuclei. For the present work, the data on the neutron multiplicity and effective temperatures as a function of E_K and M_f are used as experimental inputs to calculate fragment-neutron angular correlations for comparison with the measured fragment-neutron angular distributions as discussed below.

C. Neutron angular distributions

Experimental angular distributions of the prompt neutrons with respect to the fragment direction were determined from the analysis of the coincidence data on the grid and collector pulse height distributions. The determination of fragment angle for coincidence events follows the same procedure as for the singles events described earlier. The observed neutron angular distributions were corrected for chance coincidences arising due to background neutrons. The background contribution was estimated from the average counts in the time of flight spectrum to the left of the prompt gamma peak and to the extreme right of the neutron peak as shown by the dashed line in Fig. 2. The background level was seen to be of the order of 4% to 7% of the neutrons for events with E_K less than 180 MeV and was of the order of 9% to 15% for the events with E_K greater than 180 MeV for various fragment masses. The background corrected neutron angular distributions were obtained for various fragment mass and kinetic energy bins. The typical results on the angular distribution of neutrons for the fragment mass pair of M_L/M_H = 96/140, are shown in Fig. 4 for different E_K bins. The distributions have been plotted as a function of the cosine of the heavy fragment angle measured on either side of the ionization chamber. The absolute yields were obtained by normalizing the angle integrated neutron yield per fission for all fragments to the known value of $\overline{\nu}$= 2.42.

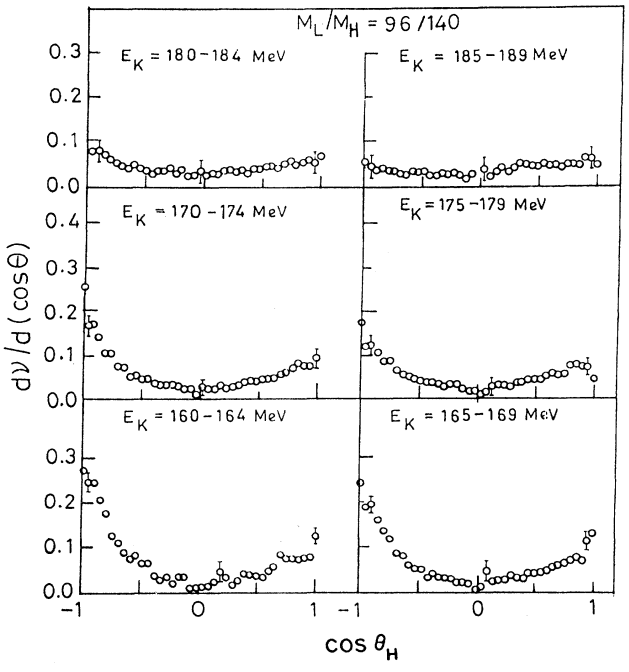

FIG. 4. Neutron angular distributions in the laboratory system as a function of the cosine of the heavy fragment angle for the mass pair of M_L= 96 amu and M_H= 140 amu for various E_K bins; error bars are shown only for a few points for the sake of clarity.

IV. CALCULATIONS

Monte Carlo calculations assuming neutron emission from fully accelerated fission fragments were carried out to determine the laboratory angular distributons of the prompt neutrons emitted from the moving fragments. The experimentally measured values of neutron multiplicities and emission spectra (T_{eff}) (Figs. 4 and 5 of Ref. [25]) were used as inputs to these calculations. The calculated neutron angular distributions correspond to neutron emission from both the fragments, whose contributions were taken in proportion to the neutron multiplicites (ν_L and ν_H) for the various E_K bins. The finite angular resolution, as experimentally determined, was folded into the Monte Carlo calculations and the change in the fragment energy due to fragment recoil because of neutron emission was also taken into account [23,26]. Since the present calculation is an event by event Monte Carlo simulation of the laboratory neutron angular distribution the recoil correction due to neutron emission which produces a change in the fragment velocity is easily incorporated in the calculation. The change in the kinetic energy of the fragments and the normalization to the singles has been taken into account while binning the neutron angular distributions for different fragment mass and kinetic energy groups. The experimentally deduced neutron detector efficiency as a function of neutron energy was also included in the calculations and only the neutrons with laboratory energy greater than the energy threshold of the neutron detector were included in the calculated neutron angular distributions.

The assumption that neutrons in the postscission stage are emitted from fully accelerated fission fragments is justified as long as the fragment acceleration time is short compared to the evaporation time of the neutrons from the fragments. As suggested by Hinde *et al.* [27], one can consider the time to attain 82% of the final fragment velocity at infinity as a measure of the time required for complete acceleration of the fragments. The fragment acceleration time and the neutron evaporation

time were calculated using the formalism given in [28]. The fragment acceleration time for 82% of final velocity is of the order of 3×10^{-21} s for the most probable fission fragment pair ($M_L/M_H = 96/140$). However, the fragments acquire major fraction ($\sim$ 50%) of their final velocity within a very short time of 10^{-21} s. The neutron evaporation time from the excited fission fragments, calculated using the fragment excitation energies of E_x = 8–15 MeV as determined from the postscission fragment neutron multiplicities and neutron energies, lie in the range of 10^{-19} to 10^{-20} s. The model calculations of [29] show that only if neutron evaporation time is comparable to the acceleration time of the fission fragments, can it lead to a decrease in the laboratory neutron anisotropy. The neutron evaporation times calculated as above are seen to be larger than the fragment acceleration time and therefore cannot lead to any significant neutron emission during fragment acceleration phase. However, a small component of neutron emission (2–3%), taking place during the very early stage of fragment acceleration is experimentally indistinguishable from the prescission neutron component.

In order to make a quantitative comparison of the measured and the calculated neutron angular distributions we have used the neutron angular anisotropies $[N(0°)/N(90°)]$ for the neutrons emitted from the individual fragments. The neutron angular anisotropies in both the forward and backward directions were determined by fitting the angular distributions to the form $(a + b\cos^2\theta)$. Some typical results of the measured neutron angular anisotropies along the direction of light and heavy fragment motion for two mass pairs (96/140 and 98/138) are shown in Fig. 5 as a function of the total kinetic energy. The sensitivity of neutron angular anisotropies to any uncertainty in the 0° and 90° calibrations was checked by changing the grid angle calibration channel numbers by an amount equivalent to the angular resolution (1.5° to 2.5°) obtained in the present measurement. It was found that these changes in the grid angular calibarations have little effect on the observed neutron angular anisotropies. It is seen from Fig. 5 that the calculated anisotropy (assuming neutron emission only from fully accelerated fragments) shows a strong increase with increasing fragment kinetic energy (as expected from kinematic focusing effects) whereas, the measured anisotropies are weakly dependent on the kinetic energy, and in certain cases even decrease at higher kinetic energies. We find that this disagreement between the calculated and the experimental anisotropy values can be removed only by incorporating a certain fraction of isotropic neutron component in the laboratory angular distributions, which we define as the prescission neutrons (ν_{pre}). The method of analysis for determination of this ν_{pre} component is described below.

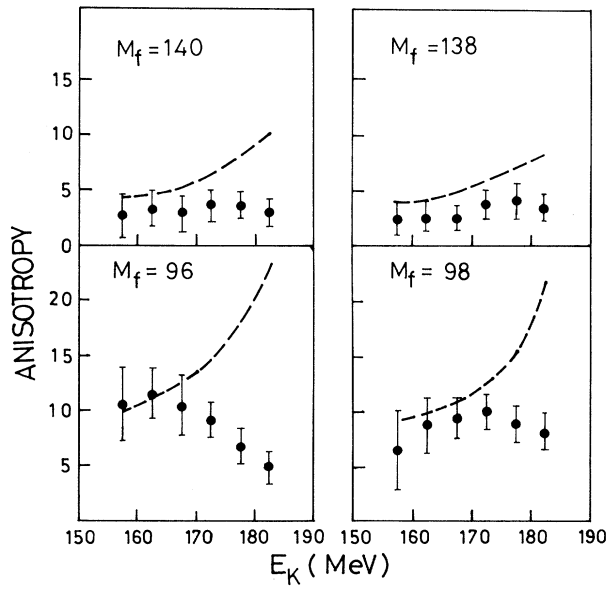

FIG. 5. Neutron angular anisotropy as a function of E_K for different fission fragment masses: •, experimental data; ———, calculation without the isotropic component.

A. Determination of prescission neutron component

The component of prescission neutrons as a function of M_f and E_K was determined by carrying out a three-source fit to the measured neutron angular distributions. The three sources were taken to be the two fission fragments moving with their full velocity and the fissioning nucleus at rest in the laboratory system. The laboratory neutron angular distributions from the fully accelerated fission fragments were calculated with the Monte Carlo technique as discussed above, and the prescission neutrons were assumed to be isotropic in the laboratory system. The multiplicities of the three components were treated as free parameters for fitting the experimentally measured neutron angular distributions for various bins of fragment M_f and E_K. Figure 6 shows the three individual components and the full fits to the measured angular distributions for the most probable mass pair for different kinetic energy bins. The values of ν_L, ν_H, and ν_{pre} obtained by the above fitting procedure are shown in Fig. 7 as a function of the fragment E_K for various average fragment masses. It is seen that for all the fragment mass pairs the postscission neutron numbers decrease as a function of E_K and approach nearly the same value for both the light and heavy fragments. However, for the mass pairs in the shell region of M_H=132 amu, the neutron multiplicities from heavy fragments are much lower than from light fragments for all kinetic energy bins.

It is also seen from the figure that the ν_{pre} values increase as a function of E_K and for large values of E_K, the values of ν_{pre} become comparable to or more than ν_L or ν_H. This result implies that for highest E_K events, neutron emission is predominantly from the prescission stage. A consequence of this result would be that for large E_K bins, the observed laboratory spectra would not reflect the usual kinematic focusing effect expected for neutrons when they are emitted from fission fragments. The energy spectra of neutrons emitted along the direc-

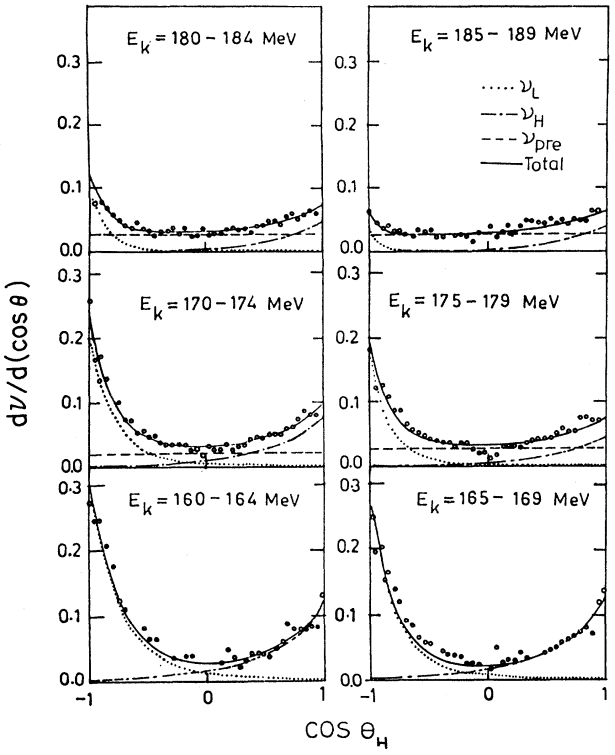

FIG. 6. Neutron angular distributions fitted to a three component fit comprising the two moving fission fragments and the fissioning nucleus —— ν_T, ····· ν_L, —·—· ν_H, - - - ν_{pre}.

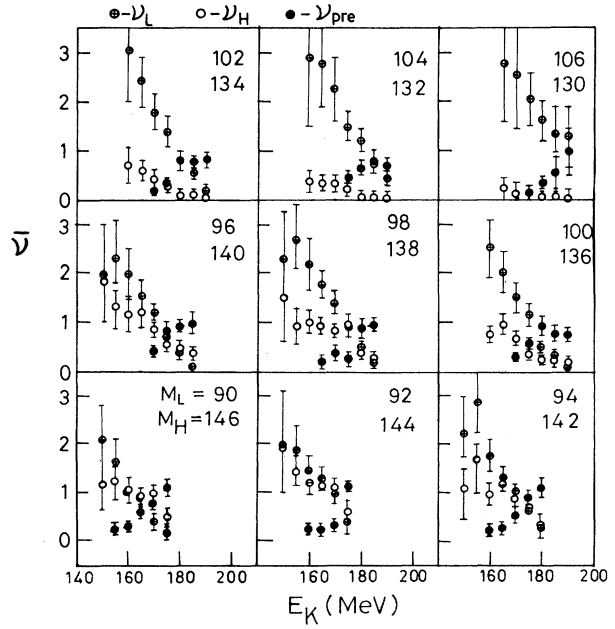

FIG. 7. $\bar{\nu}$ as a function of E_K for various fragment masses ⊕ - ν_L, o - ν_H, • - ν_{pre}.

tion of light and heavy fragments would be similar for large E_K events. To check for this behavior, we show in Fig. 8 the average values of the laboratory neutron energy spectra $[\overline{E}(0°)]$ at $0°(\pm 18°)$ in the direction of motion of the light and heavy fragments as a function of E_K for different fragment mass pairs. It is seen that, in general, the neutrons emitted along the direction of motion of the light fragments have much higher kinetic energy than those emitted along the direction of motion of the heavy fragments as expected from kinematic effects. However for the highest kinetic energy bins, the two spectra look similar as reflected by the average neutron energies in the two cases. For mass bins corresponding to heavy fragments near the doubly closed shell region of 132 amu, the neutron emission is mainly from the light fragments, and so the average energy of neutrons emitted along the light fragment direction is much higher than that in the case when the neutrons are emitted opposite to the direction of motion of the light fragment. The similarity of the neutron energy spectra in the laboratory system for neutrons emitted along the light and heavy fragment direction at large E_K values, therefore, confirms the presence of a prescission neutron component and its strong variation with fragment E_K in thermal neutron fission of ^{235}U.

The results obtained on the prescission neutron mul-

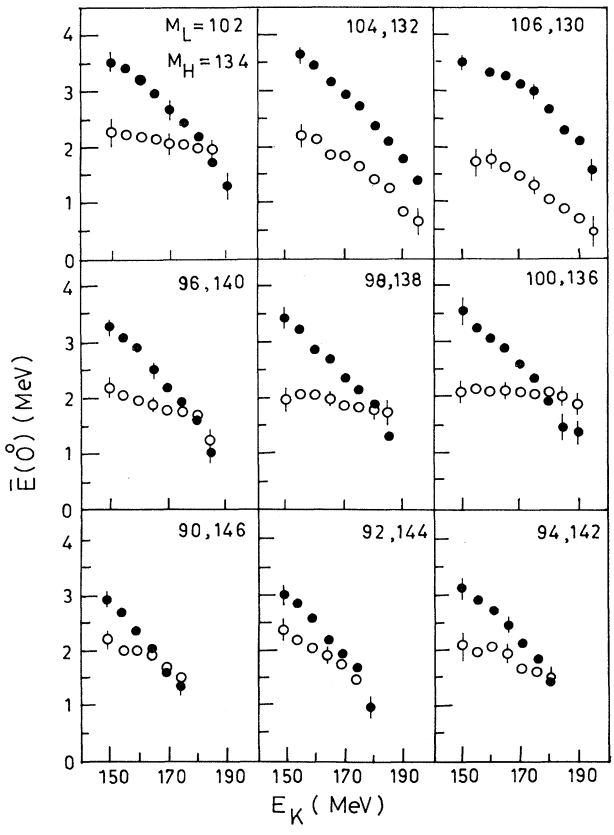

FIG. 8. Average neutron energy in the laboratory $\overline{E}(0°)$ vs E_K for various fragment masses: • - light fragments, o - heavy fragments.

tiplicity, (ν_{pre}) averaged over all E_K values are shown in Fig. 9 as a function of fragment mass. The errors shown in the data also include the uncertainties in the measurement of neutron emission spectra and multiplicities, which are used for the determination of ν_{pre} . It is seen from the figure that there is a dependence of ν_{pre} on the fragment mass; ν_{pre} is seen to be slightly higher in the doubly closed heavy fragment shell region (M_H=132, M_L=104 amu). Figure 9 also shows for comparison the total neutron multiplicity, (ν_T) as a function of fragment mass. The value of ν_{pre} averaged over all M_f and E_K bins is found to be of the order of 0.25±0.05 neutrons per fission, which amounts to about 10±2% of the total neutron emission per fission. There have been some measurements of ν_{pre} reported for the spontaneous fission of ^{252}Cf by carrying out model analysis of the neutron energy spectra, where about 1.1% of neutrons were found to be emitted in the prescission stage [34]. In the present work, a self-consistent analysis procedure is adopted to explain both the energy spectra and angular distribution of neutrons, thus providing more reliable information on the prescission neutron yields. Similar detailed analysis in the case of ^{252}Cf fission is needed to be carried out to understand the difference seen in the ν_{pre} yields for this case and for the case of thermal neutron induced fission of ^{235}U measured in the present work.

Figure 10 shows the variation of ν_{post}, ν_{pre}, and ν_T with E_K averaged over all fragment masses. It is seen that although both ν_{post} and ν_T show a decreasing trend with increasing fragment kinetic energy, ν_{pre} shows an increasing trend. The slope of the variation of ν_{post} and ν_T with E_K give the average energy required for neutron emission from the two fragments. The value of $dE_K/d\nu_T$ for the total neutron component is −18.36 MeV/neutron, whereas that for the postscission component is −12.06 MeV/neutron. The latter value is closer to what one estimates from neutron binding energy and kinetic energy considerations. The fraction of prescission neutrons

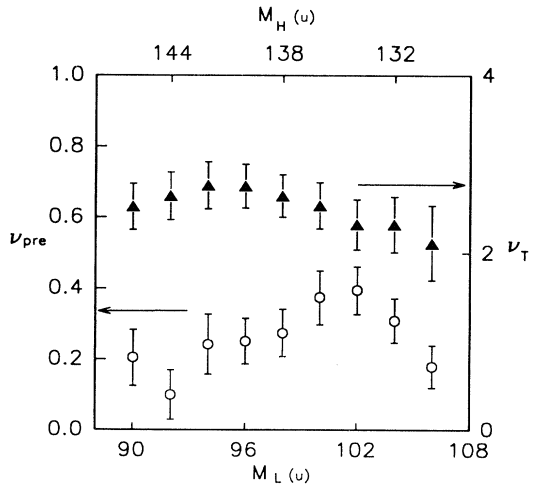

FIG. 9. ν_{pre} values as obtained from the three component fit are shown in the figure as a function of fragment mass: o, ν_{pre}, ν_T values are also shown for comparison: △, ν_T.

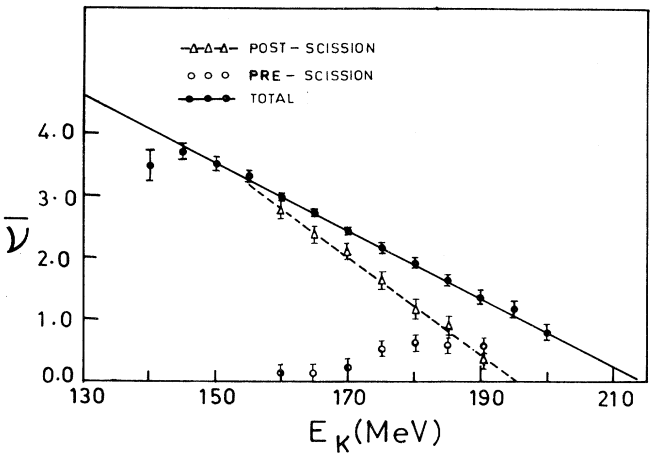

FIG. 10. $\bar{\nu}$ as a function of E_K averaged over all fragment masses: • - ν_T, △ - ν_{post}, o - ν_{pre}.

increases with increasing fragment kinetic energy. This along with the result on the variation of ν_{pre} with mass suggest that a higher fraction of isotropic neutron emission results from compact scission configurations which are likely to be observed for high E_K events as well as in the shell region of M_f = 132, where the fragment deformation energy is small.

V. DISCUSSION

The possibility of prescission neutron emission in low energy fission of heavy actinide nuclei was first speculated by Bohr and Wheeler. Dynamical theoretical calculations of Fuller [30] were done assuming the evolution of a slowly rising potential hill at the center of a square well potential which was supposed to simulate the fission process. The calculations suggested that the neutron emission probablity was dependent on the rate of development of the potential hill. Boneh *et al.* [31] also showed that scission neutron emission can take place in low energy fission with a small probability. Recent calculations [32] done assuming the nascent fission fragments as slabs of infinite nuclear matter show that there is a finite neutron emission probability from the neck region. The possibility of neutron emission during the motion of the nucleus from saddle to scission has also been postulated in some earlier studies [16]. Since the potential energy drop from saddle to scission is of the order of 30–40 MeV [33], there exists the possibility of neutron emission during the motion of the nucleus from saddle to scission. It may be noted that for heavy-ion induced fission where a much greater amount of excitation energy is deposited in the system by the projectile there is a much more pronounced yield of prescission neutrons.

The prescission neutron component in the case of thermal neutron fission can originate from the following two processes. First it is possible that a small fraction of neutrons (prescission neutrons) may be emitted during the saddle to scission motion of the fissioning nucleus due

to evaporation (ν_{ss}), when the fissioning nucleus attains a finite temperature by conversion of a fraction of the potential energy into internal excitation energy [2]. Second, it is also possible that during the very act of rupture of the neck at the moment of scission, a small fraction of neutrons may be left behind by some nonequilibrium process (scission neutrons ν_{sc}) [30].

It is possible to draw certain inferences regarding the saddle to scission time scale, if the entire prescission neutron emission is due to evaporation process during the saddle to scission stage. In the thermal neutron induced fission of ^{235}U, the excitation energy at saddle point is $\sim$ 1 MeV, and during the saddle to scission transition, there is a decrease of potential energy ($\sim$ 40 MeV) of the fissioning nucleus, which can appear in different forms such as internal excitation energy (E_x), deformation energy of the nascent fragments (E_d), and prescission kinetic energy (E_{Ko}) of the fission fragments. The division of the potential energy into E_x, E_d, and E_{Ko} depends very sensitively on the dynamics of the saddle to scission motion and the magnitude of the nuclear viscosity coefficient. Under the assumption of a large viscosity, ($E_{Ko} \sim 0$), the upper limit on E_x is 40 MeV. The saddle to scission time (τ_{ss}) was estimated from the observed average value of the prescission multiplicity ($\bar{\nu}_{\rm pre} = 0.25 \pm 0.05$) using the neutron lifetime given by the evaporation code PACE II (for the level density parameter $a = A/10$). The neutron decay width Γ_n for decay from a nucleus at excitation energy E_x is given by

$$\Gamma_n(E_x, I) = \frac{2S_n + 1}{2\pi\rho(E_x, I)} \sum_{l=0}^{\infty} \sum_{J=I-l}^{J=I+l} \times \int_0^{E_x - B_n} \rho(E_x - B_n - \epsilon_n, J) T_l(\epsilon_n) d\epsilon_n \quad (2)$$

with the associated lifetime $\tau_n = \hbar/\Gamma_n$. $\rho(E_x, I)$ is the level density at the excitation energy E_x and angular momentum I and is taken as

$$\rho(E_x, I) \propto \frac{2I + 1}{(E_x - E_{\rm rot})^2} \exp[2\sqrt{a_n(E_x - E_{\rm rot})}] , \quad (3)$$

where $E_{\rm rot}$ is the rotational energy of the nucleus at the angular momentum I, and a_n is the level density parameter for neutron. The neutron evaporation times obtained for the fissioning nucleus are much shorter than that obtained for neutron evaporation from the fission fragments. This is due to the higher excitation energy available for neutron emission in the fissioning nucleus and the rapid decrease of the neutron lifetimes with increasing available excitation energy. It is seen that for an upper limit of the excitation energy E_x=40 MeV, a value of $\tau_{ss} \sim 3.22 \times 10^{-21}$ s is required to explain the observed $\nu_{\rm pre}$ yields. However, since the available excitation energy can vary anywhere between 1 to 40 MeV, one can assume an average value of 20 MeV for the excitation energy at scission point. In this case the value of τ_{ss} is obtained to be of the order of 1.79×10^{-20} s. Classical hydrodynamical calculations [33] for nonrotating nuclei with no viscosity give fission lifetimes typically around 0.5-4.0$\times$ 10^{-21} s. Hence, it can be seen that the time scales deduced from the prescission neutron multiplicity data are larger than those expected for no viscosity. Recently there have been some attempts to determine the time scales of the heavy-ion induced fission processes in the presaddle and saddle-to-scission stages. The data of Fig. 11 have been taken from the recent result of Saxena *et al.* [35] for heavy-ion measurements of saddle to scission times. It can be seen that the time scale estimated in the present work for the case of thermal neutron fission of ^{235}U for the assumed excitation energy ($E^*_{ss} \sim$ 35–40 MeV) of the fissioning system (as shown by the dashed vertical line in Fig. 11) matches with that obtained from heavy-ion fission systematics. This implies that the fission process is overdamped, with neutron emission taking place close to the scission point, where the fissioning nucleus has maximum available excitation energy for particle evaporation.

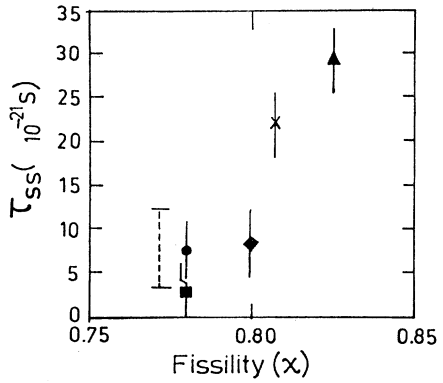

FIG. 11. Fission time scales as a function of compound nucleus fissility for compound nuclei with only saddle-to-scission time delay from heavy-ion systematics; the full lines show the limits obtained from the present result for excitation energies of 35 and 40 MeV.

The present observation of increase in $\nu_{\rm pre}$ with E_K appears significant, but a satisfactory quantitative explanation is not readily available within the above statistical model picture. The observed increase of $\nu_{\rm pre}$ with E_K may be indicative of an increase of $\nu_{\rm pre}$ for more compact configurations of the fissioning system at scission, which may be due to lower level densities for smaller deformations. This implies that, while saddle to scission times may be similar as a function of E_K, the observed increase in $\nu_{\rm pre}$ with E_K could be due to a small change in the level density parameter "a" for the compact scission configurations. However a full theoretical dynamical calculation of the saddle to scission motion is necessary to understand the present results on the prescission neutron yields as a function of fragment kinetic energy.

VI. SUMMARY

The present work reports the measurements on neutron emission spectra and angular distributions for mass

and kinetic energy selected fission fragment pairs in thermal neutron fission of ^{235}U. The measured neutron angular distributions were compared with Monte Carlo calculations for neutron emission from fully accelerated fission fragments. The calculations were done in a model independent way by using the experimentally measured neutron energy spectra and multiplicities as inputs. The measured neutron angular distributions were fitted with three neutron emission components to obtain the isotropic prescission neutron component. The prescission neutron multiplicity, ν_{pre} averaged over all fragment mass divisions was estimated to be 0.25 ± 0.05. ν_{pre} is found to be nearly the same for all fragment masses except in the region of doubly closed heavy fragment shell region, where it is somewhat larger. It is also seen that ν_{pre} shows an increase with the fragment total kinetic energy. Calculations carried out under the assumptions of the statistical model give an estimate of the time scale for saddle to scission transition which is compatible with the values obtained from heavy-ion fusion fission experiments.

ACKNOWLEDGMENTS

One of us (M.S.S.) would like to thank the Department of Atomic Energy, Board for Research in Nuclear Sciences for giving him the fellowship to do this research work.

[1] H.R. Bowman, S.G. Thomson, J.C.D. Milton, and W.J. Swiatecki, Phys. Rev. **126**, 2120 (1962).
[2] S.S. Kapoor, R. Ramanna, and P.N. Ramarao, Phys. Rev. **131**, 283 (1963).
[3] K. Skarsvag and K. Bergheim, Nucl. Phys. **45**, 72 (1963).
[4] C.P. Sargent, W. Bertozzi, P.T. Thomas, and J.L. Matthews, Phys. Rev. **137**, B89 (1965).
[5] M.V. Blinov, N.M. Kasarinov, and I.G. Krisyuk, Yad. Fiz. **12**, 41 (1970) [Sov. J. Nucl. Phys. **12**, 22 (1971)]; **16**, 1155 (1972)[**16**, 634 (1973)].
[6] C.J. Bishop, I. Halpern, R.W. Shaw, and R. Vandenbosch, Nucl. Phys. **A198**, 161 (1972).
[7] Z. Fraenkel, I. Mayk, J.P. Unik, A.J. Gorski, and W.D. Loveland, Phys. Rev. C **12**, 1809 (1975).
[8] S. Nair and D.B. Gayther, J. Phys. G **3**, 949 (1977).
[9] S. Nair, D.B. Gayther, B.H. Patrick, and E.M. Bowey, J. Phys. G **3**, 965 (1977).
[10] V.M. Piksaikin, P.P. Dyatchenko, and L.S. Kuzaeva, Yad. Fiz. **25**, 723 (1977) [Sov. J. Nucl. Phys. **25**, 385 (1977)].
[11] J.S. Samyatnin, D.K. Ryasanov, B.G. Basova, A.D. Rabinovich, and V.A. Koristilev, Yad. Fiz. **29**, 595 (1979) [Sov. J. Nucl. Phys. **29**, 305 (1979)].
[12] P. Riehs, Acta Phys. Austriaca G **53**, 271 (1981).
[13] H. Marten and D. Seeliger, in Proceedings of the International Conference on Nuclear Data for Basic and Applied Science, Santa Fe, New Mexico, 1985 (unpublished).
[14] C. Butz-Jorgensen and H.H. Knitter, Nucl. Phys. **A490**, 307 (1988).
[15] O.I. Batenkov, A.B. Blinov, M.V. Blinov, S.N. Smirnov, and V.G. Khlopin, in Proceedings of the INDC Meeting on Physics of Neutron Emission in Fission, Mito City, Japan, IAEA, INDC-(NDS)-**220**, 1989, p. 207 (unpublished).
[16] S.S. Kapoor [15], p. 221.
[17] D. Hilscher, Ann. Phys. (France) **17**, 471 (1992).
[18] R.K. Choudhury, S.S. Kapoor, D.M. Nadkarni, and P.N. Rama Rao, Nucl. Instrum. Methods **164**, 323 (1979).
[19] J. Neill, Report No. GA-9753, 1969 (unpublished).
[20] M.N. Rao, R.K. Choudhury, and S.R.S. Murthy, Nucl. Instrum. Methods Phys. Res. Sect. A **313**, 227 (1991).
[21] J.P. Unik, J.E. Gindler, L.E. Glendenin, K.F. Flynn, A. Gorski, and R.K. Sjoblom, in Proceedings of the 3rd Symposium on Physics and Chemistry of Fission, Rochester, IAEA, Vol. 2, p. 19, 1973 (unpublished).
[22] E.E. Maslin, A.L. Rodgers, and W.G.F. Core, Report No. AWRE-O-43/67, 1967 (unpublished).
[23] A. Gavron, Nucl. Instrum. Methods **115**, 99 (1974).
[24] M.S. Samant, R.P. Anand, R.K. Choudhury, D.M. Nadkarni, and S.S. Kapoor, in Proceedings of the International Conference on Nuclear Data for Science and Technology, Julich, Germany, 1991 (unpublished); Nucl. Instrum. Methods Phys. Res. Sect. A **332**, 239 (1993).
[25] M.S. Samant, R.P. Anand, R.K. Choudhury, S.S. Kapoor, K. Kumar, D.M. Nadkarni, and A. Saxena, Pramana J. Phys. **40**, 299 (1993).
[26] H. Rossner and D. Hilscher, Phys. Rev. C **43**, 2434 (1991).
[27] D.J. Hinde, R.J. Charity, G.S. Foote, J.R. Leigh, J.O. Newton, S. Ogaza, and A. Chatterjee, Nucl. Phys. **A452**, 550 (1986).
[28] V.F. Eismont, Sov. At. Energy **19**, 1000 (1965).
[29] H. Marten and D. Seeliger, J. Phys. G **14**, 211 (1988).
[30] R.W. Fuller, Phys. Rev. **126**, 684 (1962).
[31] Y. Boneh and Z. Fraenkel, Phys. Rev. C **10**, 893 (1974).
[32] P. Madler, Z. Phys. A **321**, 343 (1985).
[33] A.J. Sierk and J.R. Nix, Phys. Rev. C **21**, 982 (1980).
[34] U. Brosa and H.H. Knitter, Z. Phys. A **343**, 39 (1992).
[35] A. Saxena, A. Chatterjee, R.K. Choudhury, D.M. Nadkarni, and S.S. Kapoor, Phys. Rev. C **49**, 932 (1994).